

Quadrupole dynamics of carbon isotopes and ^{10}Be

H. Li,^{1,2,3,4} D. Fang,^{1,3} H. J. Ong,^{1,3,5,6,7} A. M. Shirokov,⁸ J. P. Vary,⁹ P. Yin,^{10,4,*} and X. Zhao^{1,3,4}

¹*Institute of Modern Physics, Chinese Academy of Sciences, Lanzhou, Gansu, 730000, China*

²*School of Nuclear Science and Technology, Lanzhou University, Lanzhou 730000, China*

³*School of Nuclear Physics, University of Chinese Academy of Sciences, Beijing, 100049, China*

⁴*CAS Key Laboratory of High Precision Nuclear Spectroscopy,*

Institute of Modern Physics, Chinese Academy of Sciences, Lanzhou 730000, China

⁵*Joint Department for Nuclear Physics, Lanzhou University and Institute of Modern Physics, Chinese Academy of Sciences, Lanzhou 730000, China*

⁶*Research Center for Nuclear Physics, Osaka University, Ibaraki, Osaka 5670047, Japan*

⁷*RIKEN Nishina Center, Wako, Saitama 351-0198, Japan*

⁸*Skobeltsyn Institute of Nuclear Physics, Lomonosov Moscow State University, Moscow 119991, Russia*

⁹*Department of Physics and Astronomy, Iowa State University, Ames, Iowa 50011, USA*

¹⁰*College of Physics and Engineering, Henan University of Science and Technology, Luoyang 471023, China*

Electric quadrupole ($E2$) moments and transitions provide measures of nuclear deformation and related collective structure. However, matrix elements of the $E2$ operator are sensitive to the nuclear wave function at large distances and are poorly convergent within the *ab initio* no-core shell model approach. We demonstrate for the first time that the ratio of neutron to proton quadrupole transition matrix elements, M_n/M_p , is well-converged in the *ab initio* no-core shell model and provides a new and robust tool for comparing with experimental results. We find that our parameter-free results for M_n/M_p for the carbon isotopes and ^{10}Be compare well with experiment, where available, and offer new insight into the quadrupole dynamics of nuclear response.

Electromagnetic and strong interaction probes of elementary particles, atomic nuclei, atoms and molecules provide precision information on their structure and dynamics. Both static and transition properties over a range of allowed multipolarities can provide detailed insights into the underlying quantum structure and dynamics of these systems. Often, these probes can be treated as perturbative in character which facilitates comparison between theory and experiment. On the other hand, for the applications in nuclear physics, it is very challenging to solve for the relevant quantities with sufficient predictive power for a quantitative comparison with experiment. We show that, for *ab initio* nuclear structure calculations, where convergence of individual long-range observables is problematic, ratios of selected observables, which involve the neutron and proton quadrupole moments, are remarkably robust and well-suited both for comparing with experiment and for predicting yet-to-be measured properties. Such demonstrations provide guidance for developing suitable robust ratios in other fields of physics.

Electric quadrupole ($E2$) observables, such as electric quadrupole moments Q_p where p represents proton, and $E2$ transition strengths $B(E2)$, reveal nuclear collective structure and dynamics [1, 2]. Since $E2$ observables are sensitive to the large-distance tails of the nuclear wave function, they are slowly convergent in *ab initio* no-core shell model (NCSM) approaches [3–6]. Even before convergence, useful predictions for static and dynamic $E2$ observables have been derived by focusing on selected ratios [7–10], rather than the absolute scale of individ-

ual $E2$ matrix elements. The prediction of $B(E2)$ values from these ratios is also found to be close to experiment data. On the other hand, in order to probe the nuclear quadrupole dynamics more completely, both proton and neutron quadrupole observables are needed and this is where strong interaction probes play a critical role [11].

The dimensionless ratios of $E2$ observables considered in this work are defined in terms of matrix elements of the quadrupole operators:

$$\begin{aligned} \frac{M_n}{M_p} &= \frac{\langle J_f || \sum_{i \in n} r_i^2 Y_2(\hat{r}_i) || J_i \rangle}{\langle J_f || \sum_{i \in p} r_i^2 Y_2(\hat{r}_i) || J_i \rangle}, \\ \frac{B(E2)}{Q_p^2} &= \frac{\langle J_f || \sum_{i \in p} r_i^2 Y_2(\hat{r}_i) || J_i \rangle^2}{\langle J_i || \sum_{i \in p} r_i^2 Y_2(\hat{r}_i) || J_i \rangle^2}, \\ \frac{M_n Q_p}{M_p Q_n} &= \frac{\langle J_f || \sum_{i \in n} r_i^2 Y_2(\hat{r}_i) || J_i \rangle \langle J_i || \sum_{i \in p} r_i^2 Y_2(\hat{r}_i) || J_i \rangle}{\langle J_f || \sum_{i \in p} r_i^2 Y_2(\hat{r}_i) || J_i \rangle \langle J_i || \sum_{i \in n} r_i^2 Y_2(\hat{r}_i) || J_i \rangle}. \end{aligned}$$

J_i (J_f) represents the total angular momentum of initial (final) state, r_i is the single-particle radius operator, and n (p) represents neutron (proton) contributions. The sensitivity of $E2$ observables to the large-distance properties of the nuclear wave function arises from the r^2 dependence of the quadrupole operators. Our focus on combinations of neutron and proton quadrupole dynamics can be viewed as extending the class of ratios of $E2$ observables shown to be valuable such as the robust convergence of $B(E2)/Q_p^2$ for ^8Li and its neighbors [9]. Additionally, previous work has shown that ratios of quadrupole moments and transition strengths to radii are well-converged in *ab initio* calculations and results up through $A = 12$ are found to be in good agreement with experiment where available [10]. It is thus reasonable to expect that M_n/M_p and $M_n Q_p / M_p Q_n$ will

* Corresponding author: pengyin@iastate.edu

also exhibit favorable convergence patterns in *ab initio* calculations with limited basis spaces.

In experiments, the M_n/M_p ratio of the quadrupole transition from 2_1^+ to the 0_1^+ ground state has been measured for several nuclei with different methods, such as ^{10}Be (proton scattering [12]); ^{10}C (proton scattering [13], $^{10}\text{C}(\alpha, \alpha')$ reaction [14]); ^{16}C ($^{16}\text{C} + ^9\text{Be}$ scattering [15], $^9\text{Be}(^9\text{Be}, 2p)$ reaction [16], proton and deuteron scattering [17]); ^{18}O (hadron scattering [18]); and ^{20}O (proton scattering [19]). The M_n/M_p for the $5/2_1^+ \rightarrow 1/2_1^+$ transition in ^{15}C has been determined via deuteron scattering [20]. The M_n/M_p ratios have received very limited theoretical attention: there are the $0\hbar\Omega$ shell model (SM) [12, 21–24] and antisymmetrized molecular dynamics (AMD) [13, 25, 26] calculations in carbon isotopes and ^{10}Be ; regarding the modern *ab initio* studies of M_n/M_p , there are only in-medium similarity renormalization group (IM-SRG) calculations for M_n/M_p in ^{16}C [17] and our previous NCSM results for ^{15}C [20] which we have recalculated and present here with a higher precision.

In this letter, we demonstrate that the ratios of M_n/M_p obtained from the *ab initio* NCSM [5, 27, 28] approach show good agreements with the available experimental data in the carbon isotopes up through $A = 16$ and ^{10}Be . Furthermore, the double ratio $M_n Q_p / M_p Q_n$, which represents the ratio of neutron and proton quadrupole matrix elements M_n/M_p over the ratio of neutron and proton quadrupole moments Q_n/Q_p , shows even better convergence than the ratio of M_n/M_p . We also find that the ratio of $B(E2)/Q_p^2$ in the carbon isotopes and ^{10}Be displays excellent convergence. The combination of experimental $B(E2)$ values and converged theoretical $B(E2)/Q_p^2$ ratios can be used to predict proton quadrupole moments. We show that the resulting proton quadrupole moment predictions are remarkably close to the results of experiments. At the same time, it is possible to make a prediction of a neutron quadrupole moment by connecting the convergent theoretical results for $M_n Q_p / M_p Q_n$ with either theoretical or experimental results for M_n/M_p and Q_p .

We perform the *ab initio* NCSM calculations with the Daejeon16 NN interaction [29] for ^{10}Be , ^{10}C , ^{11}C , ^{12}C , ^{15}C and ^{16}C , for which the experimental results of M_n/M_p and/or proton quadrupole moment are available. This interaction is based on the Entem–Machleidt N^3LO chiral effective field theory interaction [30], softened via a similarity renormalization group transformation [31] so as to provide improved convergence, and then adjusted via a phase-shift equivalent transformation to better describe nuclei with $A \leq 16$. Using the MFDn code [32, 33], we diagonalize the Hamiltonian of the system in a many-body harmonic oscillator basis which is characterized by the basis energy scale $\hbar\Omega$ and the basis truncation parameter N_{max} , the maximum number of oscillator excitation quanta allowed in the many-body space relative to the lowest Pauli-allowed configuration.

In the NCSM approach, convergence is recognized

when the calculated results become insensitive to increases in N_{max} and to variations in $\hbar\Omega$ [4].

We first consider the $E2$ strength for the $2_1^+ \rightarrow 0_1^+$ transitions in ^{10}Be , ^{10}C , ^{12}C , ^{16}C , $5/2_1^- \rightarrow 3/2_1^-$ in ^{11}C , and $5/2_1^+ \rightarrow 1/2_1^+$ in ^{15}C , shown in Fig. 1 with blue curves. While there is some tendency towards flattening of these curves with respect to $\hbar\Omega$ and compression of successive curves with respect to N_{max} , the calculated values are still changing significantly with increasing N_{max} . The dimensionless ratios of $B(E2)/Q_p^2$ yield the results shown in Fig. 1 with red curves¹. We find a near complete elimination of the $\hbar\Omega$ dependence at the highest N_{max} shown, as well as substantial compression of the curves for successive N_{max} .

The ratios of neutron and proton quadrupole matrix elements M_n/M_p for our selected transitions are in Fig. 2 with blue curves connecting calculated points. We note that the $\hbar\Omega$ dependence is less pronounced than for $B(E2)$ (Fig. 1). Moreover, the curves at higher N_{max} trend towards flattening while the spacing between curves for successive N_{max} decreases systematically. These trends indicate a progression towards converged values which agree well with the available experimental results. We also present the $M_n Q_p / M_p Q_n$ ratios as red curves in Fig. 2. Note that this ratio for ^{12}C is almost independent of N_{max} and $\hbar\Omega$ indicating a nearly complete convergence. For the transitions in the remaining nuclei considered, the ratios of $M_n Q_p / M_p Q_n$ demonstrate a more significant $\hbar\Omega$ dependence at lower N_{max} , but the curves rapidly compress and flatten at the higher N_{max} values shown.

Based on the results displayed, we make predictions of quadrupole observables from the NCSM converged ratios of $B(E2)/Q_p^2$, M_n/M_p and $M_n Q_p / M_p Q_n$. First, we consider 5 MeV $\hbar\Omega$ windows for the calculated ratios where the curves of the largest N_{max} results in each panel are approximately flat. For the ratios of $B(E2)/Q_p^2$, the windows are set from 11 to 16 MeV for ^{10}Be , and from 15 to 20 MeV for the carbon isotopes. For the ratios of M_n/M_p , the windows are set from 11 to 16 MeV for ^{10}Be , ^{10}C , ^{11}C , and from 15 to 20 MeV for ^{12}C , ^{15}C , ^{16}C . The windows are fixed from 15 to 20 MeV for the ratio of $M_n Q_p / M_p Q_n$ for all cases. Then we calculate the differences between results at the largest and the second largest N_{max} at different $\hbar\Omega$ values in this window. Finally, the computed result at the largest N_{max} corresponding to the minimum of this difference is selected as our final result, while the maximum of this difference is treated as part of the uncertainty $\Delta 1$. The second part of our uncertainty, $\Delta 2$, is from the magnitude of the difference between the results from the largest N_{max} in the selected $\hbar\Omega$ window. We adopt the sum of uncertainties of converged ratios,

¹ In calculations of ratios $B(E2)/Q_p^2$ and $M_n Q_p / M_p Q_n$ in ^{11}C we use Q_p and Q_n of the $3/2^-$ ground state; in all other nuclei we use Q_p and Q_n of excited states since their ground states have no quadrupole moments.

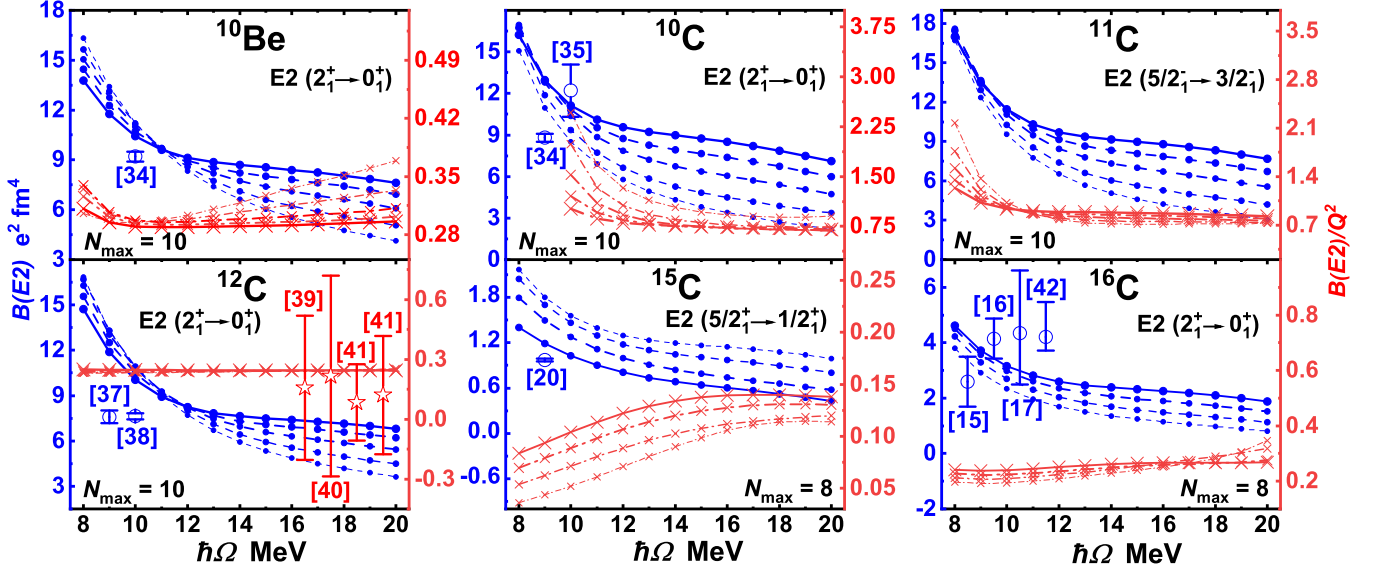


FIG. 1. (Color online) $B(E2)$ (blue and scales to the left) and the ratios $B(E2)/Q_p^2$ (red and scales to the right) in ^{10}Be , ^{10}C , ^{11}C , ^{12}C , ^{15}C , ^{16}C for the indicated transitions are shown as functions of $\hbar\Omega$. NCSM results with Daejeon16 NN interaction are shown by the dashed curves with thickness increasing with N_{max} for $N_{\text{max}} = 2, 4, 6$ for $^{15,16}\text{C}$, and $N_{\text{max}} = 2, 4, 6, 8$ for the other nuclei. The maximal N_{max} value is indicated at the bottom of each panel and is represented by the solid curves. For comparison, the available experimental $B(E2)$ and $B(E2)/Q_p^2$ data with their uncertainties are shown by open circles and stars respectively, with the citation indicated in square brackets.

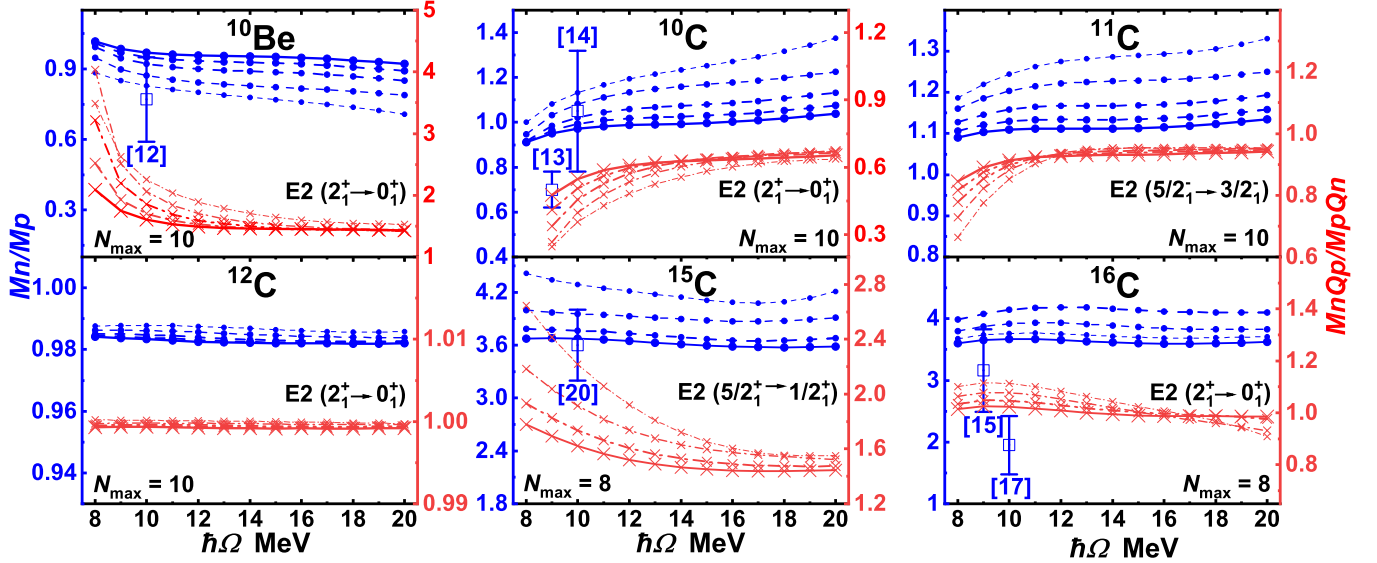


FIG. 2. (Color online) Ratios M_n/M_p (blue and scales to the left) and $M_n Q_p / M_p Q_n$ (red and scales to the right) in the same nuclei and for the same transitions as in Fig. 1. See Fig. 1 for more details. Available experimental M_n/M_p results with their uncertainties are shown by open squares with the citation indicated in square brackets.

$\Delta 1 + \Delta 2$, as the total uncertainty. Taking experimental and theoretical uncertainties into consideration, we show that the theoretical predictions (denoted by Thy) of M_n/M_p are in reasonable agreement with experimental data in Table I.

In the NCSM calculations, a crossing point is sometimes found for observables while varying N_{max} and $\hbar\Omega$.

Following established practice [8, 10, 29] we also cite these crossing points as converged results for $B(E2)$, Q_p and Q_n and mark them as Thy_{cr} in Table I. The resulting E2 strength estimations of $2_1^+ \rightarrow 0_1^+$ transition in ^{10}Be and ^{12}C are close to the experiments, while in ^{10}C the predicted $B(E2)$ value is consistent with an old experiment [35] but is approximately 30% higher

TABLE I. Predicted and experimental $B(E2)$, M_n/M_p , M_nQ_p/M_pQ_n , Q_p , and Q_n are listed along with their uncertainties. See text for the definition of column labels Thy+Exp, Thy, Thy1, and Thy_{cr}. The column Previous-Thy presents the results from previous calculations of M_n/M_p (*ab initio* IM-SRG, AMD, $0\hbar\Omega$ shell model calculations with Millener-Kurath, Warburton-Brown, Yuan-Suzuki-Otsuka-Xu interactions and using the version of the shell model suggested in Ref. [24] are labelled respectively as SM-MK, SM-WBT, SM-YSOX and SM-F).

$E2$ transitions	$B(E2)$ ($e^2 \text{ fm}^4$)		M_n/M_p			M_nQ_p/M_pQ_n		Q_p ($e \text{ fm}^2$)			Q_n (fm^2)		
	Exp	Thy _{cr}	Exp	Thy	Previous-Thy	Thy	Exp	Thy+Exp	Thy1	Thy _{cr}	Thy+Exp	Thy1	Thy _{cr}
$^{10}\text{Be}(2_1^+ \rightarrow 0_1^+)$	9.2(3) [34]	9.48(2)	1.1(1) [12]	0.96(4)	0.62(SM-MK) [12] 0.88(AMD) [26]	1.45(27)		-5.64(4)	-5.73(3)	-5.81(2)	-4.3(2)	-3.8(2)	
$^{10}\text{C}(2_1^+ \rightarrow 0_1^+)$	8.8(3) [34] 12.2(19) [35]	12.7(8)	0.70(8) [13] 1.05(27) [14]	0.98(5)	1.29(SM-MK) [21] 1.11(AMD) [13] 1.3(AMD) [25]	0.62(15)		-3.43(9) -3.9(2)	-4.1(2)		-5.8(4) -4.4(3)	-6.4(2)	-5.9(2)
$^{11}\text{C}(\frac{5}{2}_1^- \rightarrow \frac{3}{2}_1^-)$		12(1)		1.09(5)	1.19(AMD) [13]	0.93(4)	3.33(2) [36]		3.6(2)		3.9(1)	4.2(3)	3.93(2)
$^{12}\text{C}(2_1^+ \rightarrow 0_1^+)$	7.63(19) [37] 7.94(66) [38]	8.08(4)		0.982(2)	1(SM-MK) [21]	0.9992(3)	5.97(30) [37] 6(3) [39] 5.3(44) [40] 9.5(18) [41]	5.59(4) 5.71(9)	5.76(5)	5.7(2)	5.9(7) 5.9(5) 5.2(8) 9.3(2)	5.66(5)	5.6(2)
$^{15}\text{C}(\frac{5}{2}_1^+ \rightarrow \frac{1}{2}_1^+)$	0.97(2) [20]		3.6(4) [20]	3.6(2)		1.44(29)		-2.7(3)		-3.11(6)	-6.7(3)		-8.3(5)
$^{16}\text{C}(2_1^+ \rightarrow 0_1^+)$	2.6(9) [15] 4.15(73) [16] 4.34 $^{+2.27}_{-1.85}$ [17] 4.21 $^{+1.26}_{-0.50}$ [42]		3.17(67) [15] 2.4 [16] 1.95(47) [17]	3.6(2)	2.54(IM-SRG) [17] 6.07(SM-MK) [21] 2.11(SM-MK) [22] 2.47(SM-WBT) [22] 2.48(SM-YSOX) [23] 3.0(SM-F) [24] 4.19(AMD) [25]	0.99(6)		-3.12(9) -3.9(2) -4.0(5) -4.0(3)		-3.5(8)	-10(2) -9.5(3) -5.4(3)	-12.4(5)	

than suggested by a more recent experiment [34]. The prediction for $B(E2: 2_1^+ \rightarrow 0_1^+)$ in ^{12}C from the Monte Carlo Shell Model (MCSM) with Daejeon16 interaction is $7.65 e^2 \text{ fm}^4$ [43], which is in close agreement with our results.

We have not observed the crossing points of $B(E2)$ for ^{15}C and ^{16}C with current results, which may suggest that these crossings might appear at $\hbar\Omega$ and/or N_{max} values beyond the ranges of our investigation. The combination between prediction of $B(E2)/Q_p^2$ and experimental or theoretical $B(E2)$ values gives an alternative prediction of Q_p marked respectively by Thy+Exp and Thy1 in Table I.

The junction of Q_p , M_n/M_p and M_nQ_p/M_pQ_n estimation was adopted to predict another quadrupole observable, Q_n , which is essential for the understanding of proton-neutron asymmetric contributions to nuclear deformation, but is challenging to measure in experiment. The results in the Q_n column labeled as Thy+Exp were predicted from the combination of experimental and theoretical data. We used the M_n/M_p (column Exp), proton quadrupole moment (column Thy+Exp) and our results for M_nQ_p/M_pQ_n (column Thy) to make the prediction for the neutron quadrupole moments for ^{10}Be , ^{10}C , ^{15}C and ^{16}C , while our predictions of Q_n for ^{11}C and ^{12}C were obtained by making use of M_n/M_p (column Thy), experimental Q_p (column Exp) and our M_nQ_p/M_pQ_n values (column Thy). The Q_n predictions in the column Thy1 were obtained utilizing the theoretical M_n/M_p (column Thy) and Q_p (column Thy1) results.

The theoretical predictions for Q_p and Q_n (columns Thy1) are close to those obtained from the crossing points (columns Thy_{cr}). The estimations of Q_p by different methods agree well with the presented experimental re-

sults for the $3/2_1^-$ level in ^{11}C and 2_1^+ level in ^{12}C , which provides a support for our predictions of Q_p and Q_n .

In conclusion, ratios of M_n/M_p obtained from the *ab initio* NCSM approach show good agreement with available experimental data. We also provide robust *ab initio* calculations for ratios of $B(E2)/Q_p^2$ and M_nQ_p/M_pQ_n . The predicted proton quadrupole moments from the converged ratio results are close to the available experimental results. Although the neutron quadrupole moment itself is not directly accessible experimentally, *ab initio* calculations can now provide robust predictions that lead to insights into that asymmetric contributions from neutrons and protons to quadrupole deformation. By demonstrating that ratios of weakly convergent theoretical results provide robust means for comparing theory with experiment, we hope to stimulate similar investigations in other areas of physics.

We thank J. Chen and J. Li for useful discussions. J. P. Vary is supported by the US Department of Energy under Grant No. DE-SC0023692. A. M. Shirokov is supported by Chinese Academy of Sciences President's International Fellowship Initiative Grant No. 2023VMA0013. H. J. Ong is supported by the Chinese Academy of Sciences "Light of West China" Program, the National Natural Science Foundation of China under Contract Nos. 12175280 and 12250610193. X. Zhao is supported by new faculty startup funding by the Institute of Modern Physics, Chinese Academy of Sciences, by Key Research Program of Frontier Sciences, Chinese Academy of Sciences, Grant No. ZDB-SLY-7020, by the Natural Science Foundation of Gansu Province, China, Grant No. 20JR10RA067, by the Foundation for Key Talents of Gansu Province, by the Central Funds Guiding the Local Science and Technology Development of

Gansu Province, Grant No. 22ZY1QA006, by international partnership program of the Chinese Academy of Sciences, Grant No. 016GJHZ2022103FN, by National Natural Science Foundation of China, Grant No. 12375143, by National Key R&D Program of China, Grant No. 2023YFA1606903 and by the Strategic Priority Research Program of the Chinese Academy of Sciences, Grant No. XDB34000000. P. Yin is supported by the Gansu Natural Science Foundation under Grant

No. 23JRRA675. This research is supported by Gansu International Collaboration and Talents Recruitment Base of Particle Physics (2023–2027), and supported by the International Partnership Program of Chinese Academy of Sciences, Grant No. 016GJHZ2022103FN. A portion of the computational resources were also provided by Gansu Computing Center and Gansu Advanced Computing Center.

-
- [1] A. Bohr and B. R. Mottelson, *Nuclear Structure, vol. II* (World Scientific, Singapore, 2010).
- [2] D. J. Rowe, *Nuclear Collective Motion: Models and Theory* (World Scientific, Singapore, 2010).
- [3] S. K. Bogner, R. J. Furnstahl, P. Maris, R. J. Perry, A. Schwenk, and J. P. Vary, Convergence in the no-core shell model with low-momentum two-nucleon interactions, *Nucl. Phys. A* **801**, 21 (2008).
- [4] P. Maris and J. P. Vary, *Ab initio* nuclear structure calculations of *p*-shell nuclei with JISP16, *Int. J. Mod. Phys. E* **22**, 1330016 (2013).
- [5] B. R. Barrett, P. Navrátil, and J. P. Vary, *Ab initio* no core shell model, *Prog. Part. Nucl. Phys.* **69**, 131 (2013).
- [6] D. Odell, T. Papenbrock, and L. Platter, Infrared extrapolations of quadrupole moments and transitions, *Phys. Rev. C* **93**, 044331 (2016).
- [7] A. Calci and R. Roth, Sensitivities and correlations of nuclear structure observables emerging from chiral interactions, *Phys. Rev. C* **94**, 014322 (2016).
- [8] M. A. Caprio, P. J. Fasano, P. Maris, and A. E. McCoy, Quadrupole moments and proton-neutron structure in *p*-shell mirror nuclei, *Phys. Rev. C* **104**, 034319 (2021).
- [9] M. A. Caprio and P. J. Fasano, *Ab initio* estimation of $E2$ strengths in ${}^8\text{Li}$ and its neighbors by normalization to the measured quadrupole moment, *Phys. Rev. C* **106**, 034320 (2022).
- [10] M. A. Caprio, P. J. Fasano, and P. Maris, Robust *ab initio* prediction of nuclear electric quadrupole observables by scaling to the charge radius, *Phys. Rev. C* **105**, L061302 (2022).
- [11] A. M. Bernstein, V. R. Brown, and V. A. Madsen, Neutron and Proton Matrix Elements for Low-Lying 2^+ Transitions and the Probe Dependence of the Nuclear Deformation Parameter, *Comments Nucl. Part. Phys.* **11**, 203 (1983).
- [12] H. Iwasaki *et al.*, Quadrupole deformation of ${}^{12}\text{Be}$ studied by proton inelastic scattering, *Phys. Lett. B* **481**, 7 (2000).
- [13] C. Jouanne *et al.*, Structure of low-lying states of ${}^{10,11}\text{C}$ from proton elastic and inelastic scattering, *Phys. Rev. C* **72**, 014308 (2005).
- [14] T. Furuno *et al.*, Neutron quadrupole transition strength in ${}^{10}\text{C}$ deduced from the ${}^{10}\text{C}(\alpha, \alpha')$ measurement with the MAIKo active target, *Phys. Rev. C* **100**, 054322 (2019).
- [15] H. J. Ong *et al.*, Lifetime measurements of first excited states in ${}^{16,18}\text{C}$, *Phys. Rev. C* **78**, 014308 (2008).
- [16] M. Wiedeking *et al.*, Lifetime measurement of the first excited 2^+ state in ${}^{16}\text{C}$, *Phys. Rev. Lett.* **100**, 152501 (2008).
- [17] Y. Jiang *et al.* (RIBLL Collaboration), Quadrupole deformation of ${}^{16}\text{C}$ studied by proton and deuteron inelastic scattering, *Phys. Rev. C* **101**, 024601 (2020).
- [18] A. M. Bernstein, V. R. Brown, and V. A. Madsen, Isospin decomposition of nuclear multipole matrix elements from γ decay rates of mirror transitions: Test of values obtained with hadronic probes, *Phys. Rev. Lett.* **42**, 425 (1979).
- [19] J. Jewell *et al.*, Proton scattering on the radioactive nucleus ${}^{20}\text{O}$ and the $0^+_{gs} \rightarrow 2^+$ transition in the neutron-rich oxygen isotopes, *Phys. Lett. B* **454**, 181 (1999).
- [20] J. Chen *et al.*, Probing the quadrupole transition strength of ${}^{15}\text{C}$ via deuteron inelastic scattering, *Phys. Rev. C* **106**, 064312 (2022).
- [21] H. Sagawa, X. R. Zhou, X. Z. Zhang, and T. Suzuki, Deformations and electromagnetic moments in carbon and neon isotopes, *Phys. Rev. C* **70**, 054316 (2004).
- [22] C. Yuan, C. Qi, and F. Xu, Shell evolution in neutron-rich carbon isotopes: Unexpected enhanced role of neutron-neutron correlation, *Nucl. Phys. A* **883**, 25 (2012).
- [23] C. Yuan, T. Suzuki, T. Otsuka, F. Xu, and N. Tsunoda, Shell-model study of boron, carbon, nitrogen, and oxygen isotopes with a monopole-based universal interaction, *Phys. Rev. C* **85**, 064324 (2012).
- [24] H. T. Fortune, $B(E2)$ values in neutron-excess nuclei near $A = 16$, *Phys. Rev. C* **93**, 044322 (2016).
- [25] Y. Kanada-En'yo, Proton dominance in the $2^+_2 \rightarrow 0^+_1$ transition of $N = Z \pm 2$ nuclei around ${}^{28}\text{Si}$, *Phys. Rev. C* **84**, 024317 (2011).
- [26] Y. Kanada-En'yo, Y. Shikata, Y. Chiba, and K. Ogata, Neutron dominance in excited states of ${}^{26}\text{Mg}$ and ${}^{10}\text{Be}$ probed by proton and α inelastic scattering, *Phys. Rev. C* **102**, 014607 (2020).
- [27] P. Navrátil, J. P. Vary, and B. R. Barrett, Large basis *ab initio* no-core shell model and its application to ${}^{12}\text{C}$, *Phys. Rev. C* **62**, 054311 (2000).
- [28] P. Navrátil, J. P. Vary, and B. R. Barrett, Properties of ${}^{12}\text{C}$ in the *ab initio* nuclear shell model, *Phys. Rev. Lett.* **84**, 5728 (2000).
- [29] A. M. Shirokov, I. J. Shin, Y. Kim, M. Sosonkina, P. Maris, and J. P. Vary, N3LO NN interaction adjusted to light nuclei in *ab exitu* approach, *Phys. Lett. B* **761**, 87 (2016).
- [30] D. R. Entem and R. Machleidt, Accurate charge dependent nucleon-nucleon potential at fourth order of chiral perturbation theory, *Phys. Rev. C* **68**, 041001 (2003).
- [31] S. K. Bogner, R. J. Furnstahl, and R. J. Perry, Similarity Renormalization Group for Nucleon-Nucleon Interactions, *Phys. Rev. C* **75**, 061001 (2007).

- [32] P. Maris, M. Sosonkina, J. P. Vary, E. Ng, and C. Yang, Scaling of ab-initio nuclear physics calculations on multicore computer architectures, *Procedia Computer Science* **1**, 97 (2010), iCCS 2010.
- [33] H. M. Aktulga, C. Yang, E. G. Ng, P. Maris, and J. P. Vary, Improving the scalability of a symmetric iterative eigensolver for multi-core platforms, *Concurrency and Computation: Practice and Experience* **26**, 2631 (2013).
- [34] E. A. McCutchan *et al.*, Lifetime of the 2_1^+ state in ^{10}C , *Phys. Rev. C* **86**, 014312 (2012).
- [35] T. R. Fisher, S. S. Hanna, D. C. Healey, and P. Paul, Lifetimes of Levels in $A = 10$ Nuclei, *Phys. Rev.* **176**, 1130 (1968).
- [36] N. J. Stone, Table of nuclear electric quadrupole moments, *Atom. Data Nucl. Data Tabl.* **111-112**, 1 (2016).
- [37] A. D'Alessio *et al.*, Precision measurement of the $E2$ transition strength to the 2_1^+ state of ^{12}C , *Phys. Rev. C* **102**, 011302 (2020).
- [38] B. Pritychenko, M. Birch, B. Singh, and M. Horoi, Tables of $E2$ Transition Probabilities from the first 2^+ States in Even-Even Nuclei, *Atom. Data Nucl. Data Tabl.* **107**, 1 (2016).
- [39] W. Vermeer, M. Esat, J. Kuehner, R. Spear, A. Baxter, and S. Hinds, Electric quadrupole moment of the first excited state of ^{12}C , *Phys. Lett. B* **122**, 23 (1983).
- [40] M. Kumar Raju *et al.*, Reorientation-effect measurement of the first 2^+ state in ^{12}C : confirmation of oblate deformation, *Phys. Lett. B* **777**, 250 (2018).
- [41] J. Saiz-Lomas *et al.*, The spectroscopic quadrupole moment of the 2_1^+ state of ^{12}C : A benchmark of theoretical models, *Phys. Lett. B* **845**, 138114 (2023).
- [42] M. Petri *et al.*, Structure of ^{16}C : Testing shell model and *ab initio* approaches, *Phys. Rev. C* **86**, 044329 (2012).
- [43] T. Otsuka, T. Abe, T. Yoshida, Y. Tsunoda, N. Shimizu, N. Itagaki, Y. Utsuno, J. Vary, P. Maris, and H. Ueno, α -Clustering in atomic nuclei from first principles with statistical learning and the Hoyle state character, *Nature Commun.* **13**, 2234 (2022).